JOINT EUROPEAN TORUS

JET–P(91)24

M.A. Kovanen
and JET Team

Monte-Carlo Study of High Power (D)T ICRF Heating in JET

Monte-Carlo Study of High Power (D)T ICRF Heating in JET

M A. Kovanen and JET Team*

JET-Joint Undertaking, Culham Science Centre, OX14 3DB, Abingdon, UK

Lappeenranta University of Technology, Finland and National Research Council for Technology, The Academy of Finland
** See Appendix 1*

Preprint of Paper to be submitted for publication in
Nuclear Fusion

Monte-Carlo Study of High Power (D)T ICRF Heating in JET

M.A. Kovanen*

JET Joint Undertaking, Abingdon, Oxon. OX14 3EA, U.K.

Abstract

A Monte-Carlo investigation of the high power fundamental minority (D)T ICRF heating in JET is undertaken. The effect of the minority ion concentration, the location of the resonance layer, the symmetry of the wave field spectrum, the background ion temperature and the α-particle absorption of the ICRF power on the fusion yield is assessed in a projected pellet injected reference discharge ($n_e(0) = 10^{20}m^{-3}$, $T_e(0)$ =12 keV, $T_i(0)$ = 10 keV, P_{rf} = 25 MW, $(P_D + P_\alpha)_{abs}/P_{rf}$ = 80%). Even with $n_D/n_e \sim 30\%$, which is needed for high fusion yield, the finite orbit width and its related transport effects, such as the banana drift, and the RF induced diffusion and drift, are important and strongly reduce the attainable yield. However, as here the transferred power to background ions dominates over the power to electrons, the increased target triton temperature can significantly improve the yield, and achieving Q (= P_{fus}/P_{rf}) = 1 in JET would appear to be feasible. The use of the asymmetric wave field spectrum improves the confinement of the resonating ions and is shown to substantially enhance the yield and the duration time of the peak yield value. This effect,if also applied to tritons, could delay the characteristic deterioration of the peaked density profiles during the pellet-enhanced-performance (PEP) modes. α-particle absorption of the RF power was found to be very small.

1. Introduction

Radiofrequency heating in the ion cyclotron range of frequencies (ICRF) has been shown to enhance fusion reactivity beyond what is expected for Maxwellian distributions. Experiments of ICRF (^{3}He)D heating in JET have produced fast, MeV range, particles and a ^{3}He-D fusion yield $P_{fus} \approx$ 140 kW [1]. Furthermore, Stix calculated fusion reactions from

---

*Lappeenranta University of Technology, Finland and National Research Council for Technology, The Academy of Finland

minority deuterium at $\omega = \omega_{CD}$ with a Fokker-Planck model, and concluded that the fusion multiplication factor Q (= P_{fus}/P_{rf}) could be made greater than one [2]. Thus, the (D)T ICRF scheme has great potential, and its experimental investigation has also been proposed for the JET D-T phase [3]. Predictions for this scheme in JET suggest that effective deuterium damping, up to 80%, could be achieved even with high minority concentrations $n_D/n_T \leq 40\%$, and that the (D)T yield could be as high as 17 MW (P_{rf} = 25 MW, Z_{eff} = 2) [4]. However, it has been shown that the finite orbit width and its related transport processes, such as the banana drift, and the RF induced diffusion and drift, can significantly alter the RF power absorption, power transfer to background electrons and ions, and thermonuclear yield profiles, particularly in high power ICRF minority heating cases [5]. This coincides with the fact that the zero orbit width approximation has typically produced higher fusion yield estimates than the experiments would indicate [6]. Modelling of the finite orbit effects has recently been done using the Stix model together with a simplified set of equations to describe the particle trajectories [7]. The effects of the neoclassical and RF driven transport processes, and the E_- wave electric field component were neglected.

In this study a full Monte-Carlo simulation of high power (P_{rf} = 25 MW) fundamental (D)T ICRF heating in JET is undertaken using the orbit following code HECTOR [8]. The effect of the minority ion concentration, location of the resonance layer, and symmetry of the wave field spectrum on the fusion yield is assessed, and the feasibility to achieve Q = 1 in JET investigated. As there is concern that the α-particles, which have the same resonance frequency as deuterium and a large Doppler broadening, might effectively absorb RF power in the outer region of the plasma [9], the effect of α-particles on ICRF heating is also included. The pellet-enhanced-performance (PEP) mode combined with the H-mode during the ICRF heating has produced a high fusion reactivity in JET [10]. As the PEP regime may become important for reactor ignition studies, a projected high power pellet injected (peaked profile) discharge is used as a reference discharge.

2. Numerical Assumptions

HECTOR is a Monte Carlo code which follows the trajectories of test particles (~ 2000) in an axisymmetric tokamak plasma. The particles, which initially have a Maxwellian velocity distribution, are described with an orbit integrated source function in the C.O.M. phase space. The particle interaction with the RF wave fields and the Coulomb collision processes of dynamical friction, pitch angle scattering and energy diffusion are included. The magnetic field topology was here calculated from a model [11], which represents the JET plasma equilibria. A description of HECTOR and some of its previous applications can be found in [5,8,12,13].

The plasma is assumed to be in a steady state, with the plasma density and temperature profiles modelled with a parabolic form

$$y(x) = [y(o) - y(a)]\left(1 - x^2\right)^{\nu} + y(a), \tag{1}$$

where y(a), y(o) represent the edge and central values, respectively, and ν is the profile parameter. The single-pass absorption for a fixed value of $k_{\|} = 7\ m^{-1}$ is assumed to have a deuterium damping efficiency $P_{D,abs}/P_{rf} = 80\%$. The input profile for the RF power absorption density is given in a form

$$< P_{abs}(Z) > = < P_{abs}(o) > \exp(-2LZ^2), \tag{2}$$

where Z is the distance from the median plane in the vertical direction and L is the electric field profile parameter.

The plasma parameters of the pellet-injected (peaked profile) reference discharge are shown in Table I. The discharge is assumed to have $Z_{eff} = 1.0$. As the impurity influx does not change the amount of fuel and the burn-up fraction is low, the temporal increase in Z_{eff} can, thus, be neglected here. The flow of thermal particles to the plasma centre replacing the diffused and drifted high energy particles is included with the neoclassical transport processes.

The α-particle effects were included by doing parallel simulations, where the α-particle yield from (D)T ICRH was used as the particle source in the (α)T ICRF calculation. The total absorbed RF power ($= P_D + P_\alpha)_{abs}$ was kept constant.

3. Results and Discussion

The fusion yield is shown in Fig. 1 as a function of the RF resonance position. While the maximum P_{fus} is obtained in the zero orbit width limit at $r \cong 0.3$ m [4], the orbit calculation for the same case gives the maximum at $r \cong 0.15$ m in the absence of the E_- component of the wave electric field. The optimum deuterium tail temperature $T_i \cong 140$keV, which can be used in the zero orbit calculations, is not reached when the finite orbit width and its related transport processes are included. Furthermore, the maximum yield was not found at the highest temperature as there the deterioration of the peaked minority density profile is the largest. When the E_- term is included, although the higher tail temperature indicates a shift in the resonance position outwards, a further reduction in the central minority density results in the optimum resonance position being located at $r \cong 0.10$m. The reduction in the P_{fus} at $r \cong 0.3$ m due to the finite orbit effects is ~ 20% without the E_- term, and ~ 40% with the E_- term. Thus, even with such high minority concentration, orbit effects are clearly important. Furthermore, due to the transport the maximum value of the P_{fus} cannot be sustained for a long period of time unless the minority density in the centre is replenished (Fig. 2). The neoclassical transport of thermal ions to the plasma centre is not strong enough to prevent the falling off in the yield from its peak value after $t = 0.25\tau_s$, where τ_s is the Spitzer slowing down time.

The minority ion concentration strongly affects the Q value (Fig. 3). This value is seen to increase with the minority concentration and to reach its maximum value of ~ 0.75 at $n_D/n_e \cong 0.35$. At higher concentrations the fusion yield and the Q value are reduced as the shielding decreases the power absorption by the minority ions and power is absorbed by other mechanisms such as direct electron heating by TTMP and electron Landau damping.

The use of the asymmetric wave field spectrum with positive parallel wave numbers $k_{||}$ has been shown to significantly improve the minority ion confinement [5]. The pump-out of the high energy minority ions from the centre of the discharge is substantially reduced and the mean energy of the resonating ions can be sustained closer to the value of the maximum fusion reactivity (Fig. 4). The tail energy is raised as the losses of those particles, which have gained energy from the RF wave fields, are reduced. The asymmetric wave field spectrum with

positive $k_{||}$ not only improves the fusion yield compared with the cases with the symmetric spectrum, but also extends the period during which the maximum P_{fus} can be maintained. This is demonstrated in Fig. 5 neglecting the decay of the triton density profile. In Fig. 6 the fusion yield is compared using the symmetric and asymmetric wave field spectra for various $k_{||}$ values. A substantial difference in P_{fus} even at low $k_{||}$ values and at high minority concentrations is seen. However, obtaining Q = 1 by modifying the wave spectrum may not be sufficient on its own as the RF absorption efficiency by the minority ions suffers at high $k_{||}$ values.

As the mean energy of the minority ions remains moderate, the fusion reactivity is strongly affected by the triton target temperature. In Fig. 7 it is shown that even using the symmetric wave field spectrum, increasing the peak ion temperature to ~ 18 keV would be sufficient for reaching the Q = 1, and at 25 keV Q would be 1.4. So far in the JET ICRH experiments the central ion temperatures in high density plasmas have typically been in the region of 10 keV. In these experiments, however, the small minority ion concentration $\leq 5\%$ has resulted in very high tail temperatures, in the the MeV range, where the power has been transferred primarily to electrons. In our projected case the mean energy of the resonating ions stays low enough for the ion heating to dominate (Fig. 8). Thus, scaling the target ion temperature from the existing data for our reference case would underestimate the obtainable T_i. In view of this (and taking into account the benefits of using an asymmetric wave spectrum), achieving Q = 1.0 in JET appears to be feasible.

As the increase in the triton target temperature has such a profound effect on the fusion yield, it may be worth considering the use of some of the RF power for direct triton heating with an asymmetric wave spectrum. Although the termination of the PEP-modes is associated with such processes as the MHD activity [14], the direct triton heating, in addition to raising the target temperature, would improve the plasma ion confinement and delay the characteristic decay of the peaked density profiles during these modes.

The effect of the α-particle absorption on the ICRF heating efficiency was found to be very small. Although the high energy α-particles have an efficient ICRF absorption they will be quickly lost from the region of the peak wave field strength due to the strong orbit width

related transport. This transport is stronger for the α-particles than for the deuterium minority as it depends on the particle energy. Furthermore, the overall number of α-particles produced remains small even after a considerably long time. After τ_s the α-particle absorption had only risen to 350 kW using the symmetric wave spectrum ($k_{||} = \pm 7$ m^{-1}) and up to 400 kW with the asymmetric spectrum ($k_{||} = +7$ m^{-1}).

Summary

A Monte-Carlo study of the high power (D)T ICRH heating in JET has been undertaken using a projected pellet injected (peaked profile) discharge. It is shown, that even with ~30% minority concentration, where the tail temperature remains moderate, the orbit width and its related transport processes play an important role reducing considerably the obtainable fusion yield. At this high deuterium concentration strong background ion heating occurs and less power is transferred to electrons. The consequent increase in triton target temperature will significantly increase the yield and achieving Q = 1 in JET would appear to be feasible. The asymmetric wave field spectrum with positive parallel wave numbers improves the confinement of the resonating ions. Thus, the yield is significantly enhanced and the fall off in the yield as seen with the symmetric wave spectrum cases does not occur. Furthermore, this effect, particularly if applied also to tritons, could delay the strong deterioration of the peaked density profiles during the PEP-modes. The absorption of the RF power by the α-particles was found to be very small. The concentration of the α-particles in the centre of the discharge stays small due to a weak burn-up and the effective transport.

Acknowledgement

It is a pleasure to thank W.G.F. Core, G.A. Cottrell, L.-G. Eriksson, T. Hellsten, D.F.H. Start and A. Taroni for fruitful discussions, JET Theory Division for hospitality, and the Finnish Cultural Foundation for financial support.

References

[1] The JET Team (presented by Stott, P.E.), Recent Results from JET, The 32nd Meeting of the Division of Plasma Physics of the American Physical Society, Cincinnati (1990).

[2] Stix, T.H., Nuclear Fusion 15 (1975) 737.

[3] JET Team, Plas. Phys. and Contr. Fusion 30 (1988) 1467.

[4] Cottrell, G.A., et al., Plas. Phys. and Contr. Fusion 31 (1989) 1727.

[5] Kovanen, M.A., Core, W.G.F., Hellsten, T., Finite Orbit Effects in ICRF Heated Tokamak Plasmas, JET Joint Undertaking, JET-P(90)68, submitted for publication in Nucl. Fusion.

[6] Eriksson, L.-G., Hellsten, T., Boyd, D.A., et al., Nucl. Fusion 29 (1989) 87.

[7] Cottrell, G.A., Start, D.F.H., Nucl. Fusion 31 (1991) 61.

[8] Kovanen, M.A., Core, W.G.F., HECTOR - A Code for the Study of Charged Particles in Axisymmetric Tokamak Plasmas, JET Joint Undertaking, JET-P(90)40, submitted for publication in J. Comput. Phys.

[9] Hellsten, T., Appert, K., Vaclavik, J., Villard, L., Nuclear Fusion 25 (1985), 99.

[10] Tubbing, B.J.D., Balet, B., Bartlett, D.V., et al., H-Mode Confinement in JET with Enhanced Performance by Pellet-Peaked Density Profiles, JET Joint Undertaking, JET-P(90)67, submitted for publication in Nucl. Fusion.

[11] Stringer, T., An Analytic Model for the Poloidal Field in JET, JET Joint Undertaking, JDN/T(83)6 (1983).

[12] Kovanen, M.A., Reichle, R., Lazzaro, E., Summers, D.D.R., Taylor, T., Modelling of the Observed Particle and Heat Fluxes in the X-Point Region at JET, JET Joint Undertaking, JET-P(91)06, submitted for publication in Nucl. Fusion.

[13] Cordey, J.G., Christiansen, J.P., Core, W.G.F., et al., Electron Heating in JET by ICRH, to be presented at the 18th EPS Conference on Controlled Fusion and Plasma Physics, Berlin (1991).

[14] Kupschus, P., Balet, B., Bartlett, D., et al., High Thermonuclear Yield on JET by Combining Enhanced Plasma Performance of ICRH-Heated, Pellet-Peaked Density

Profiles with H-Mode Confinement, to be presented at the 18th EPS Conference on Controlled Fusion and Plasma Physics, Berlin (1991).

TABLE I

Plasma Parameters for the Reference Discharge

Coupled RF power, P_{rf}	25 MW
Damped RF power on minority ions, $(P_D+P_\alpha)_{abs}$	20 MW
Central electron density, $n_e(0)$	$1 \times 10^{20} m^{-3}$
Central electron temperature, $T_e(0)$	12 keV
Central ion temperatures, $T_i(0)$	10 keV
Density profile parameter, ν_n	4.0
Temperature profile parameter, ν_T	2.0
Deuterium-to-electron density ratio, n_D/n_e	30%
Plasma major radius, R_o	2.96 m
Plasma minor radius, a	1.2 m
Central magnetic field $B_\phi(R_o)$	3.3 T
Plasma current , I_p	3.0 MA
Perpendicular wave number, $k_\perp$	$25 m^{-1}$
Parallel wave number, $k_\parallel$	$7 m^{-1}$
RF frequency, f	21.7-27.3MHz
Electric field profile parameter, L	12.5

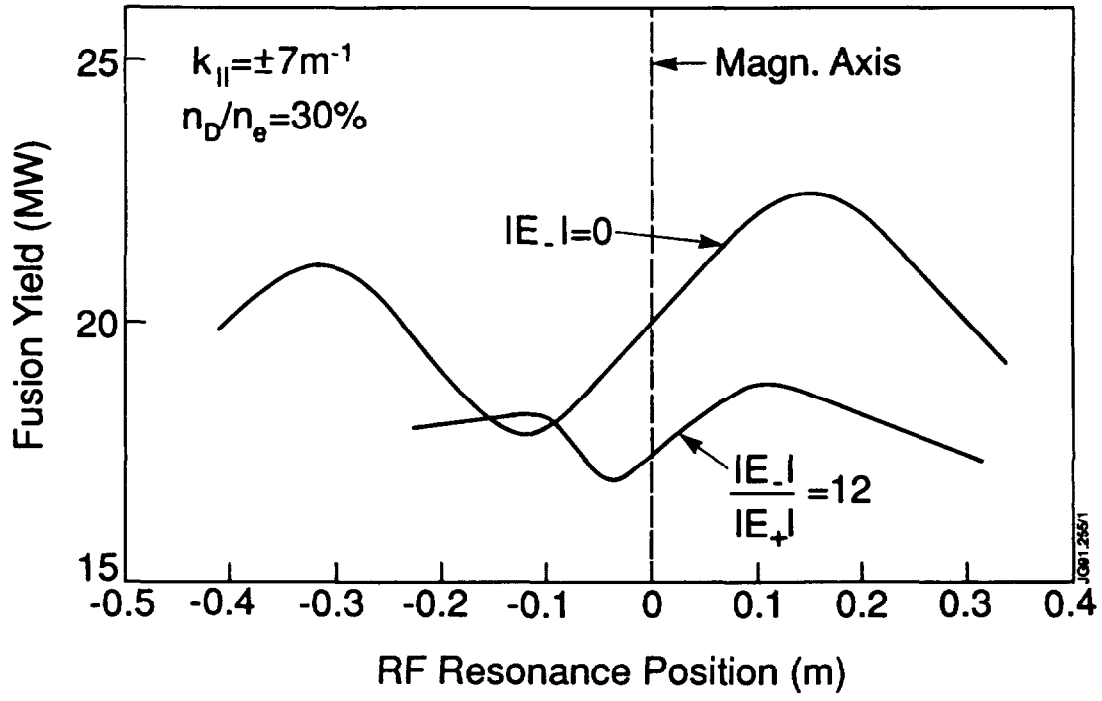

Fig. 1 Fusion yield as a function of the RF resonance position.

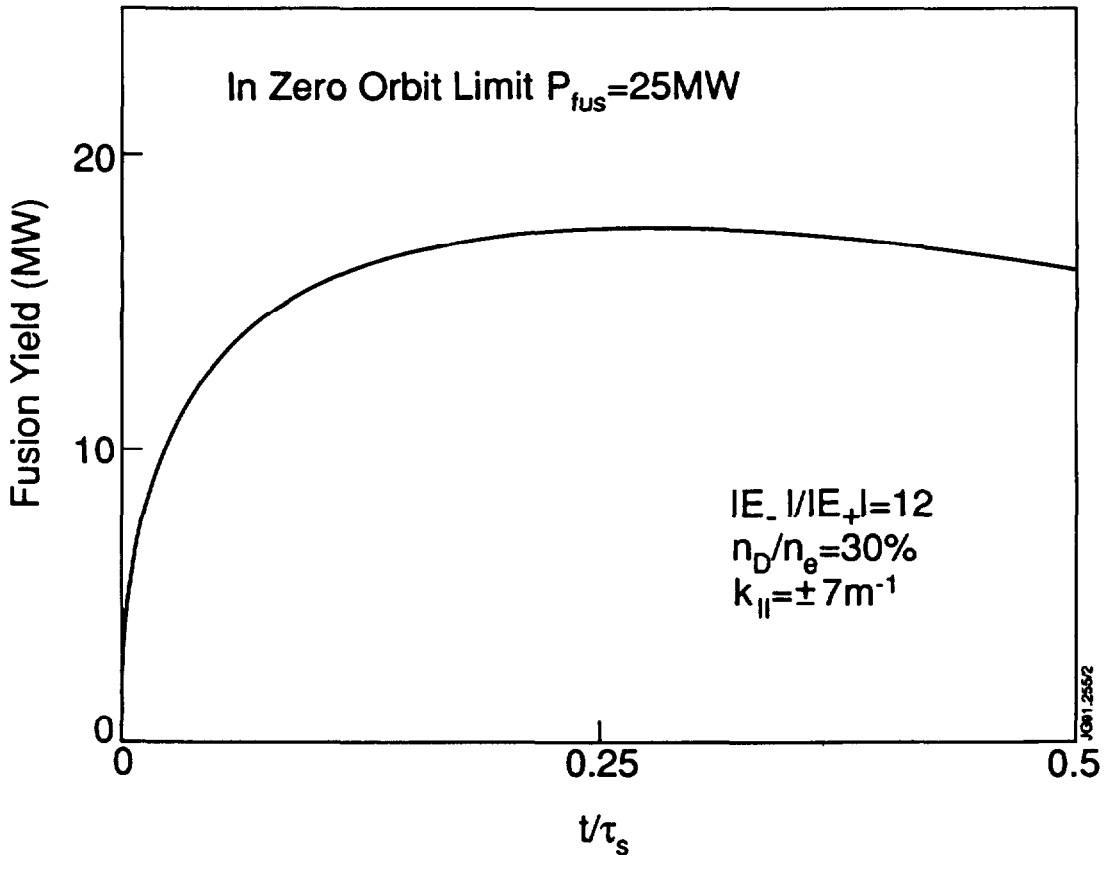

Fig. 2 The temporal behaviour of the fusion yield at the resonance position r = 0.3m.

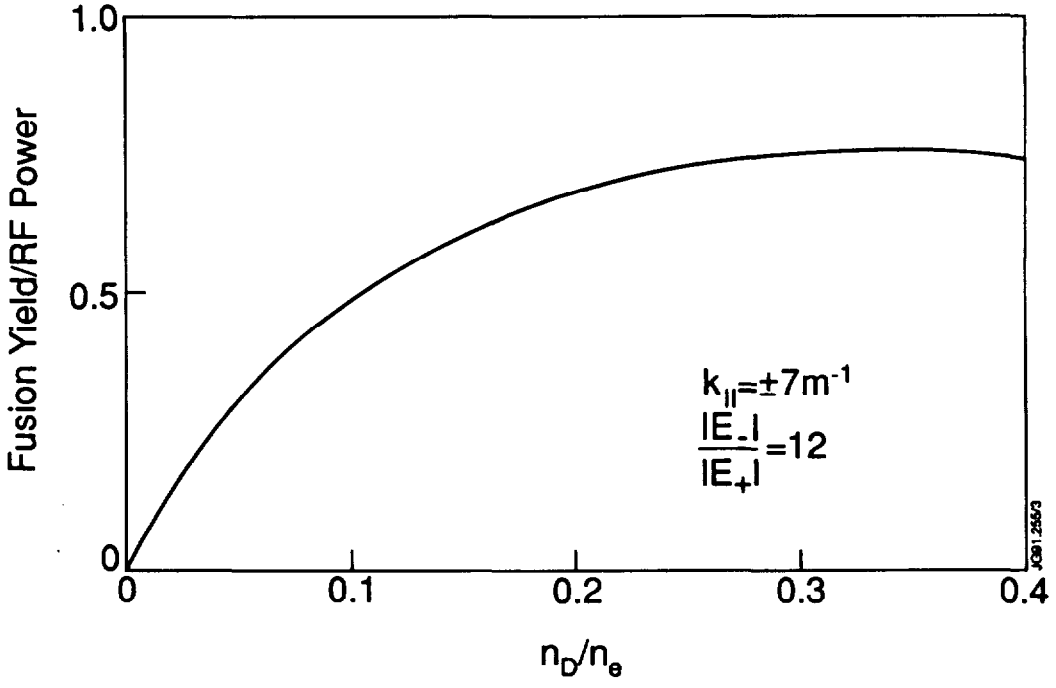

Fig. 3 The effect of the minority ion concentration on the fusion multiplication factor. The resonance position is at r = 0.1m.

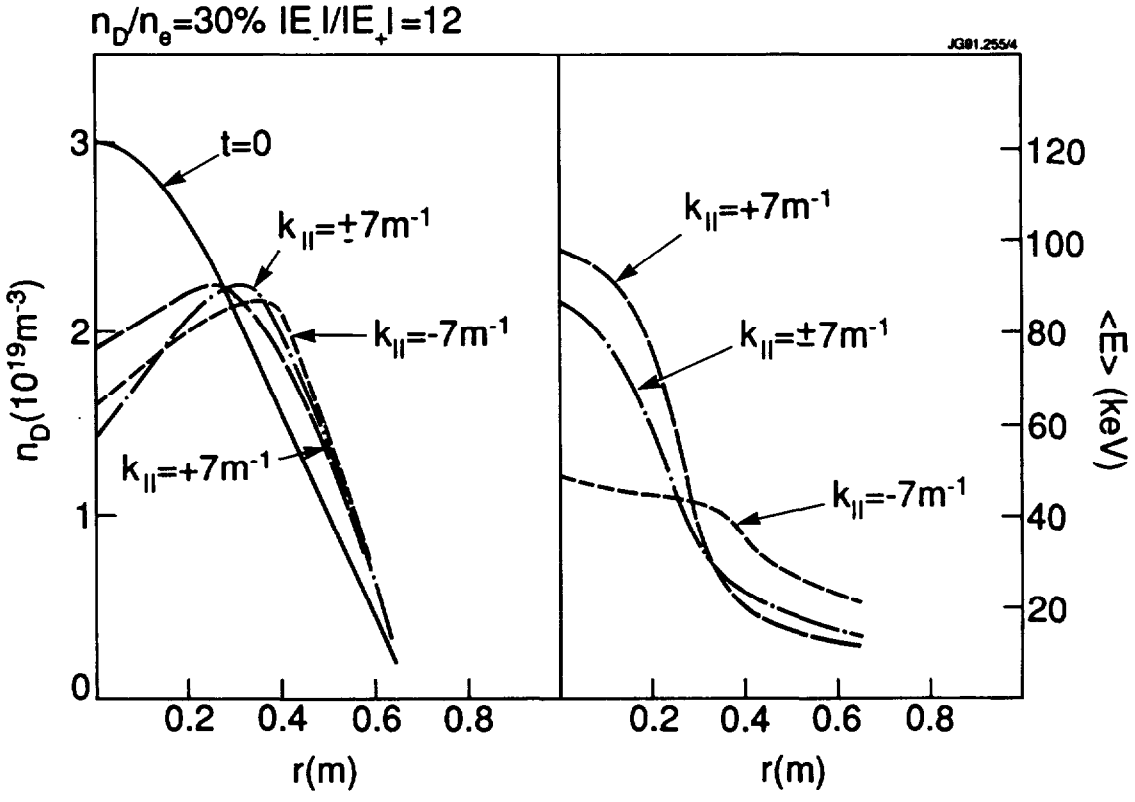

Fig. 4 The radial density and mean energy profiles of the minority ions at t = 0.25 τ_s with the symmetric ($k_{||}$ = ± 7m) and asymmetric ($k_{||}$ = - 7m and $k_{||}$ = + 7m) wave field spectra. The resonance position is at r = 0.1m.

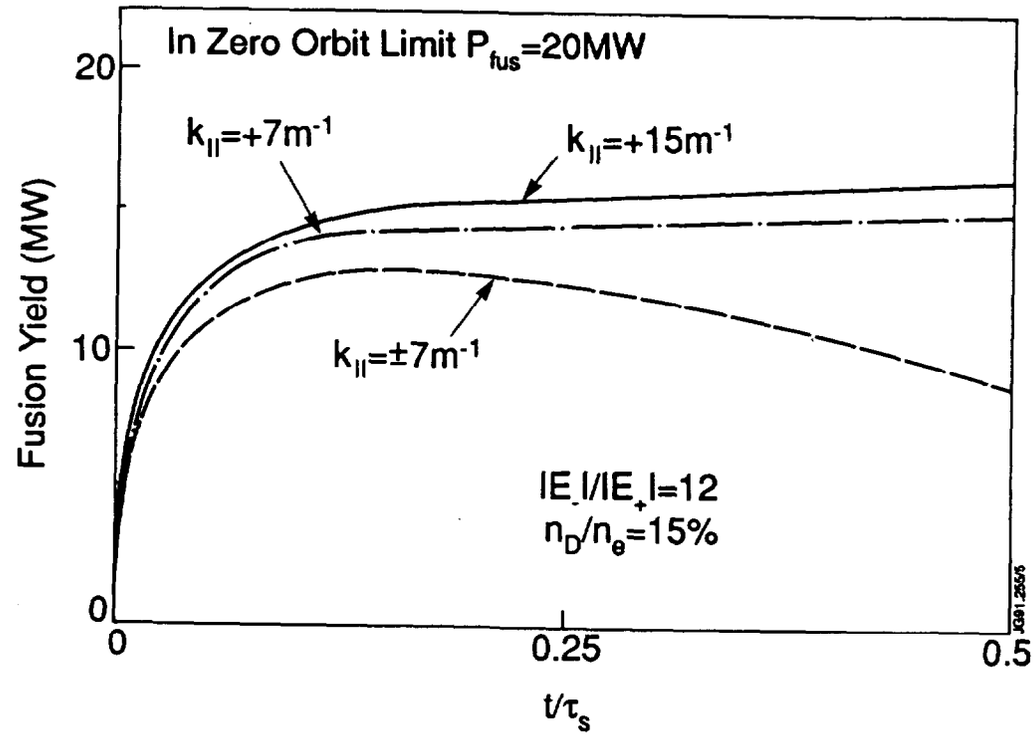

Fig. 5 The behaviour of the fusion yield for the symmetric ($k_{||} = \pm 7$m) and asymmetric ($k_{||} = +7$m, $k_{||} = +15$m) wave field spectra. The resonance position is at r = 0.1m.

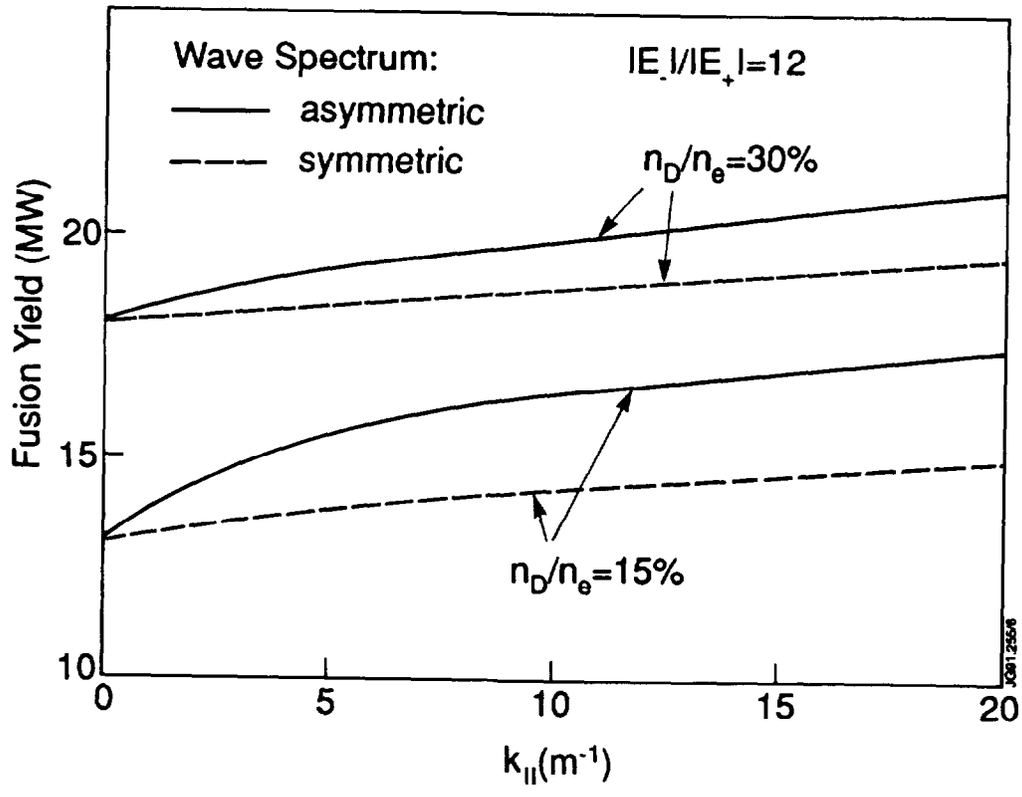

Fig. 6 The fusion yield as a function of the parallel wave number at t = 0.25 τ_s. The resonance position is at r = 0.1m.

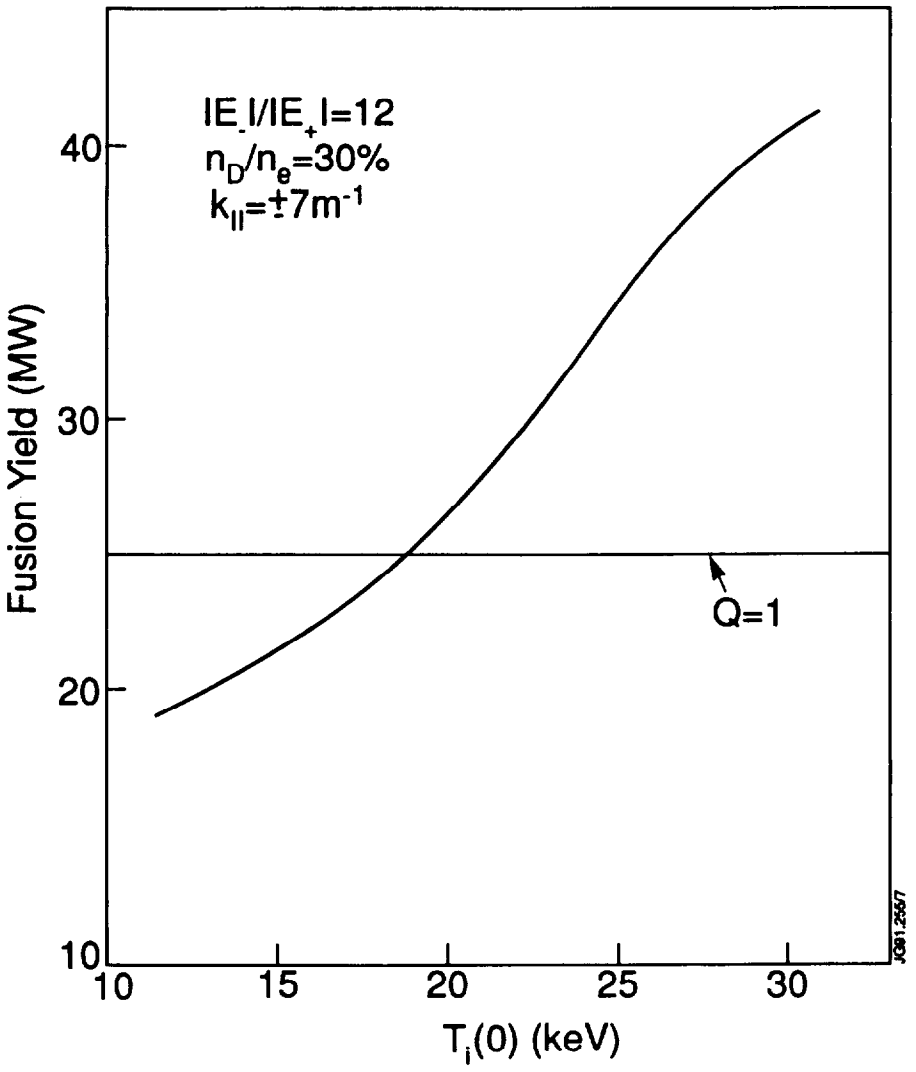

Fig. 7 The effect of the background ion temperature on the fusion yield. The calculation is at $t = 0.25\ \tau_s$. The symmetric wave field spectrum was used at the resonance position r=0.1m.

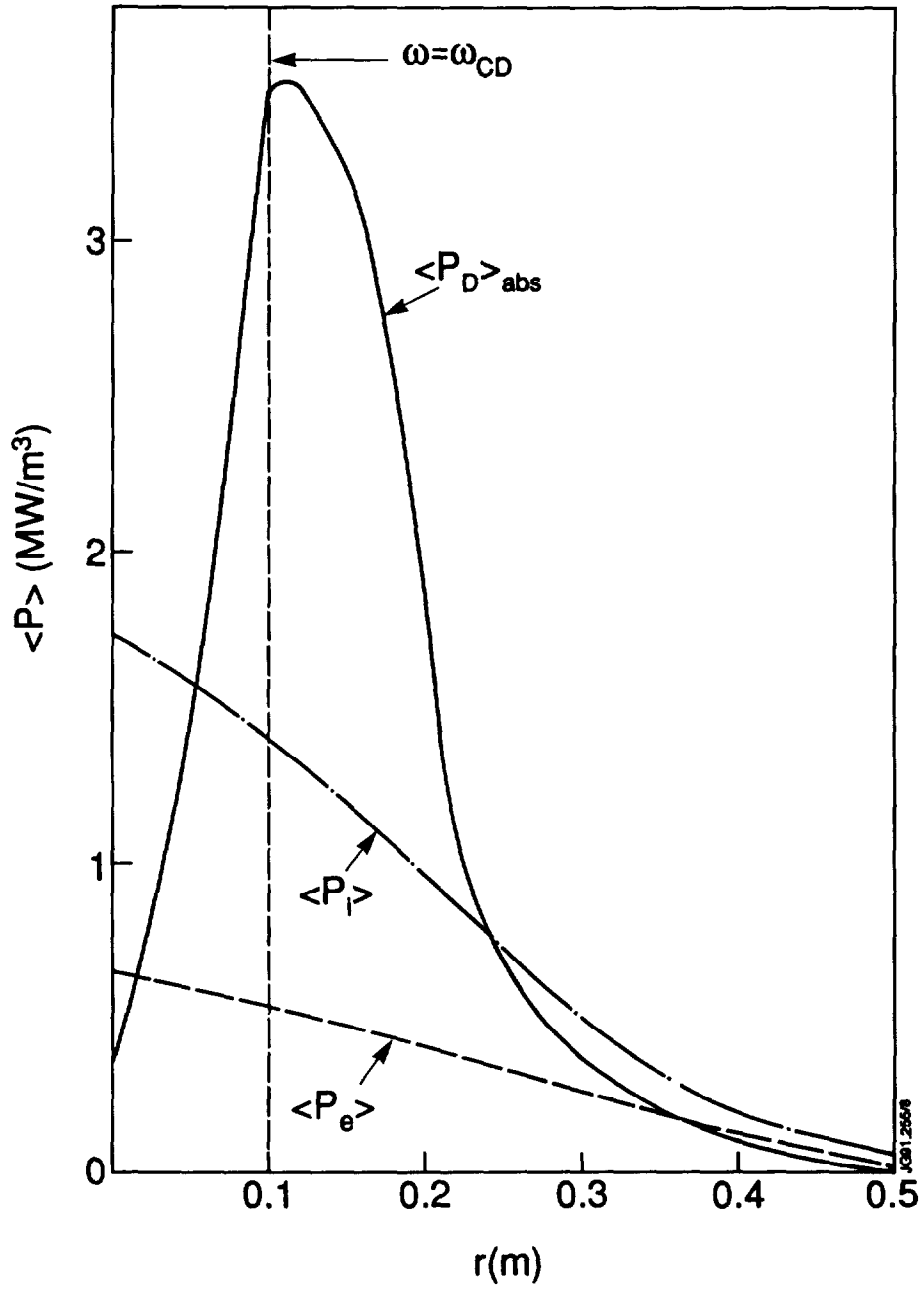

Fig. 8 The radial power density profiles for the RF absorption, $\langle P_D \rangle_{abs}$, and background electron and ion heating rates, $\langle P_e \rangle$, $\langle P_i \rangle$ at $t = 0.25\ \tau_s$. The asymmetric wave field spectrum was used at the resonance position of r = 0.1m.

APPENDIX 1.

THE JET TEAM

JET Joint Undertaking, Abingdon, Oxon, OX14 3EA, U.K.

J.M.Adams[1], F.Alladio[4], H.Altmann, R.J.Anderson, G.Appruzzese, W.Bailey, B.Balet, D.V.Bartlett, L.R.Baylor[24], K.Behringer, A.C.Bell, P.Bertoldi, E.Bertolini, V.Bhatnagar, R.J.Bickerton, A.Boileau[3], T.Bonicelli, S.J.Booth, G.Bosia, M.Botman, D.Boyd[31], H.Brelen, H.Brinkschulte, M.Brusati, T.Budd, M.Bures, T.Businaro[4], H.Buttgereit, D.Cacaut, C.Caldwell-Nichols, D.J.Campbell, P.Card, J.Carwardine, G.Celentano, P.Chabert[27], C.D.Challis, A.Cheetham, J.Christiansen, C.Christodoulopoulos, P.Chuilon, R.Claesen, S.Clement[30], J.P.Coad, P.Colestock[6], S.Conroy[13], M.Cooke, S.Cooper, J.G.Cordey, W.Core, S.Corti, A.E.Costley, G.Cottrell, M.Cox[7], P.Cripwell[13], F.Crisanti[4], D.Cross, H.de Blank[16], J.de Haas[16], L.de Kock, E.Deksnis, G.B.Denne, G.Deschamps, G.Devillars, K.J.Dietz, J.Dobbing, S.E.Dorling, P.G.Doyle, D.F.Düchs, H.Duquenoy, A.Edwards, J.Ehrenberg[14], T.Elevant[12], W.Engelhardt, S.K.Erents[7], L.G.Eriksonn[5], M.Evrard[2], H.Falter, D.Flory, M.Forrest[7], C.Froger, K.Fullard, M.Gadeberg[11], A.Galetsas, R.Galvao[8], A.Gibson, R.D.Gill, A.Gondhalekar, C.Gordon, G.Gorini, C.Gormezano, N.A.Gottardi, C.Gowers, B.J.Green, F.S.Griph, M.Gryzinski[26], R.Haange, G.Hammett[6], W.Han[9], C.J.Hancock, P.J.Harbour, N.C.Hawkes[7], P.Haynes[7], T.Hellsten, J.L.Hemmerich, R.Hemsworth, R.F.Herzog, K.Hirsch[14], J.Hoekzema, W.A.Houlberg[24], J.How, M.Huart, A.Hubbard, T.P.Hughes[32], M.Hugon, M.Huguet, J.Jacquinot, O.N.Jarvis, T.C.Jernigan[24], E.Joffrin, E.M.Jones, L.P.D.F.Jones, T.T.C.Jones, J.Källne, A.Kaye, B.E.Keen, M.Keilhacker, G.J.Kelly, A.Khare[15], S.Knowlton, A.Konstantellos, M.Kovanen[21], P.Kupschus, P.Lallia, J.R.Last, L.Lauro-Taroni, M.Laux[33], K.Lawson[7], E.Lazzaro, M.Lennholm, X.Litaudon, P.Lomas, M.Lorentz-Gottardi[2], C.Lowry, G.Magyar, D.Maisonnier, M.Malacarne, V.Marchese, P.Massmann, L.McCarthy[28], G.McCracken[7], P.Mendonca, P.Meriguet, P.Micozzi[4], S.F.Mills, P.Millward, S.L.Milora[24], A.Moissonnier, P.L.Mondino, D.Moreau[17], P.Morgan, H.Morsi[14], G.Murphy, M.F.Nave, M.Newman, L.Nickesson, P.Nielsen, P.Noll, W.Obert, D.O'Brien, J.O'Rourke, M.G.Pacco-Düchs, M.Pain, S.Papastergiou, D.Pasini[20], M.Paume[27], N.Peacock[7], D.Pearson[13], F.Pegoraro, M.Pick, S.Pitcher[7], J.Plancoulaine, J-P.Poffé, F.Porcelli, R.Prentice, T.Raimondi, J.Ramette[17], J.M.Rax[27], C.Raymond, P-H.Rebut, J.Removille, F.Rimini, D.Robinson[7], A.Rolfe, R.T.Ross, L.Rossi, G.Rupprecht[14], R.Rushton, P.Rutter, H.C.Sack, G.Sadler, N.Salmon[13], H.Salzmann[14], A.Santagiustina, D.Schissel[25], P.H.Schild, M.Schmid, G.Schmidt[6], R.L.Shaw, A.Sibley, R.Simonini, J.Sips[16], P.Smeulders, J.Snipes, S.Sommers, L.Sonnerup, K.Sonnenberg, M.Stamp, P.Stangeby[19], D.Start, C.A.Steed, D.Stork, P.E.Stott, T.E.Stringer, D.Stubberfield, T.Sugie[18], D.Summers, H.Summers[20], J.Taboda-Duarte[22], J.Tagle[30], H.Tamnen, A.Tanga, A.Taroni, C.Tebaldi[23], A.Tesini, P.R.Thomas, E.Thompson, K.Thomsen[11], P.Trevalion, M.Tschudin, B.Tubbing, K.Uchino[29], E.Usselmann, H.van der Beken, M.von Hellermann, T.Wade, C.Walker, B.A.Wallander, M.Walravens, K.Walter, D.Ward, M.L.Watkins, J.Wesson, D.H.Wheeler, J.Wilks, U.Willen[12], D.Wilson, T.Winkel, C.Woodward, M.Wykes, I.D.Young, L.Zannelli, M.Zarnstorff[6], D.Zasche[14], J.W.Zwart.

PERMANENT ADDRESS

1. UKAEA, Harwell, Oxon. UK.
2. EUR-EB Association, LPP-ERM/KMS, B-1040 Brussels, Belgium.
3. Institute National des Récherches Scientifique, Quebec, Canada.
4. ENEA-CENTRO Di Frascati, I-00044 Frascati, Roma, Italy.
5. Chalmers University of Technology, Göteborg, Sweden.
6. Princeton Plasma Physics Laboratory, New Jersey, USA.
7. UKAEA Culham Laboratory, Abingdon, Oxon. UK.
8. Plasma Physics Laboratory, Space Research Institute, Sao José dos Campos, Brazil.
9. Institute of Mathematics, University of Oxford, UK.
10. CRPP/EPFL, 21 Avenue des Bains, CH-1007 Lausanne, Switzerland.
11. Risø National Laboratory, DK-4000 Roskilde, Denmark.
12. Swedish Energy Research Commission, S-10072 Stockholm, Sweden.
13. Imperial College of Science and Technology, University of London, UK.
14. Max Planck Institut für Plasmaphysik, D-8046 Garching bei München, FRG.
15. Institute for Plasma Research, Gandhinagar Bhat Gujat, India.
16. FOM Instituut voor Plasmafysica, 3430 Be Nieuwegein, The Netherlands.
17. Commissiariat à L'Energie Atomique, F-92260 Fontenay-aux-Roses, France.
18. JAERI, Tokai Research Establishment, Tokai-Mura, Naka-Gun, Japan.
19. Institute for Aerospace Studies, University of Toronto, Downsview, Ontario, Canada.
20. University of Strathclyde, Glasgow, G4 ONG, U.K.
21. Nuclear Engineering Laboratory, Lapeenranta University, Finland.
22. JNICT, Lisboa, Portugal.
23. Department of Mathematics, Univeristy of Bologna, Italy.
24. Oak Ridge National Laboratory, Oak Ridge, Tenn., USA.
25. G.A. Technologies, San Diego, California, USA.
26. Institute for Nuclear Studies, Swierk, Poland.
27. Commissiariat à l'Energie Atomique, Cadarache, France.
28. School of Physical Sciences, Flinders University of South Australia, South Australia SO42.
29. Kyushi University, Kasagu Fukuoka, Japan.
30. Centro de Investigaciones Energeticas Medioambientales y Techalogicas, Spain.
31. University of Maryland, College Park, Maryland, USA.
32. University of Essex, Colchester, UK.
33. Akademie de Wissenschaften, Berlin, DDR.

CR 88.49.1A